Geocarto International

ISSN: (Print) (Online) Journal homepage: https://www.tandfonline.com/loi/tgei20

# Detection and analysis of drought over Turkey with remote sensing and model-based drought indices

Behnam Khorrami & Orhan Gündüz

**To cite this article:** Behnam Khorrami & Orhan Gündüz (2022) Detection and analysis of drought over Turkey with remote sensing and model-based drought indices, Geocarto International, 37:26, 12171-12193, DOI: 10.1080/10106049.2022.2066197

**To link to this article:** https://doi.org/10.1080/10106049.2022.2066197

Published online: 25 Apr 2022.

GEOCARTO INTERNATIONAL
2022, VOL. 37, NO. 26, 12171–12193
https://doi.org/10.1080/10106049.2022.2066197

Taylor & Francis
Taylor & Francis Group

Check for updates

# Detection and analysis of drought over Turkey with remote sensing and model-based drought indices

Behnam Khorrami[a] and Orhan Gündüz[b]

[a]Department of GIS, The Graduate School of Applied and Natural Sciences, Dokuz Eylul University, Buca, Izmir, Turkey; [b]Department of Environmental Engineering, Faculty of Engineering, Izmir Institute of Technology, Izmir, Turkey

**ABSTRACT**

Under the severe impacts of climate change, drought has become one of the most undesirable and complex natural phenomena with critical consequences for the environment, economy and society. The orthodox drought monitoring approaches use observations of meteorological stations, which are typically restricted in time and space. Remote sensing, conversely, provides continuous global coverage of a variety of hydro-meteorological variables that are influential in drought, and data extracted from remote sensing and modeling missions are now considered more practical and alluring for researchers. In this study, we applied a combination of field data, remotely sensed data and modeled data to detect and quantitatively analyze drought phenomena. To achieve this objective, we utilized Terrestrial Water Storage Anomalies (TWSA) estimations from GRACE mission, Normalized Difference Vegetation Index (NDVI) from MODIS mission, Surface Runoff (R) and Evapotranspiration from ERA5 reanalysis datasets and Soil Moisture (SM) from GLDAS data model to evaluate their feasibility in detecting recent droughts over Turkey. We validated the accuracy of several remote sensing-based indices (GRACE Drought Severity Index, Water Storage Deficit Index [WSDI], Soil Moisture Index, Standardized Runoff Index and NDVI) with the traditional indices (SPI and SPEI) calculated from *in situ* observations of precipitation. The results revealed that the GRACE-based WSDI gave the best performance with high correlations with the SPI index both temporally and spatially over Turkey. We also found that monthly and annual time series of WSDI agreed well with the SPI index with correlations of 0.69 and 0.73, respectively. The results of drought analysis also indicated that WSDI could be used as a proxy to standard meteorological drought indices over Turkey as it performed well to detect and characterize the recent droughts of Turkey based on its comparisons to SPI results.

**ARTICLE HISTORY**
Received 5 June 2021
Accepted 10 April 2022

**KEYWORDS**
Drought; GRACE; water storage deficit index; drought severity index; Turkey

## 1. Introduction

Being characterized by terrestrial water deficit (Sun et al. 2018), drought is an undesirable and complex environmental phenomenon with severe environmental and socio-economic

**CONTACT** Orhan Gündüz orhangunduz@iyte.edu.tr

consequences (Hosseini-Moghari and Araghinejad 2015). According to Wilhite (2005), droughts can be classified into four major types based on their causes: (i) meteorological drought (precipitation loss), (ii) agricultural drought (soil moisture loss), (iii) hydrological drought (surface runoff, total water and groundwater loss) and (iv) socioeconomic drought (water supply and demand loss). However, since precipitation is the main input of the water cycle, all droughts can be associated with precipitation deficiency and/or evapotranspiration (ET) anomaly. The most direct and obvious manifestation of drought is reflected in surface and subsurface water resources. Due to the variations in the global patterns of climatic variables, particularly temperature and precipitation, drought is now becoming a recurrent natural catastrophe, especially in arid and semi-arid regions of the world. Compared to other natural hazards, drought has added destructive power because of its harsh impacts on different aspects of nature and human life especially when it is prolonged and extensive (Brown et al. 2008). Hence, detection and monitoring of droughts bear critical importance to provide a means for better management of the limited water supplies (Khorrami and Gündüz 2019).

The growing amount of space missions during the recent decades has led to the increased number of remote sensing (RS) datasets, which provided multiple data sources for environmental studies. Remotely sensed data and indices as well as modeled variables are used to evaluate different types of droughts all over the world. For instance, vegetation indices such as Normalized Difference Vegetation Index (NDVI) (Gu et al. 2007; Klisch and Atzberger 2016), Vegetation Condition Index (VCI) (Dutta et al. 2015), Vegetation Temperature Condition Index (VTCI) (Xie et al. 2017), Soil Moisture data (Souza et al. 2021), runoff data (Sattar et al. 2020) are among the most applied drought-related variables in monitoring and assessing drought conditions in different parts of the world.

One of the recent advances in the RS world is indeed the emergence of The Gravity Recovery and Climate Experiment (GRACE) twin satellite mission, which initiated its task in March 2002. The mission's main goal is to collect gravitational signals of the Earth and interpret them into the variations of total/terrestrial water storage (TWS) (Ramillien et al. 2008). TWS is a key element of the hydrological water cycle whose variations are used in different hydro-climatic studies ranging from oceanography to hydrology. GRACE data have also been used for drought monitoring and water storage analysis all over the world (Li et al. 2012; Cui et al. 2019; Shah and Mishra 2020; Dharpure et al. 2020). The findings of these studies suggest that there is no universal GRACE-based drought index suitable to be applied in any study area around the world. While some studies find a specific method quite useful and efficient, others cast doubt on the efficiency of that method in another area, potentially due to the geographic as well as climatic characteristics of the area of interest. In particular, drought detection and monitoring are challenging because the spatio-temporal variability of drought events and associated hydro-climatic parameters as well as the characteristics of basins make it literally impossible to formulate and use a universally applicable drought indicator (Smakhtin and Hughes 2007). Therefore, analysis and evaluation of different drought-related parameters have been a common research agenda for many researchers around the world during their search for an appropriate drought index for a particular region.

Being mostly situated in a semi-arid zone, Turkey also faces numerous challenges regarding its water resources. To date, droughts in Turkey have been evaluated through several studies. As examples of the recent studies, Sönmez et al. (2005) investigated droughts by using SPI and concluded that the severity of the recent droughts had been critical over the Central Anatolian region. Simsek and Cakmak (2010) evaluated the impacts of the 2007–2008 agricultural drought in Turkey and reported that the Southeastern Anatolia region had experienced the second most severe drought of the last 69 years in 2007–2008 with a harsh impact on the agricultural activities of the region and serious decreases in yields. Dabanlı et al. (2017) performed an investigation into the long-term variability of droughts in Turkey. They suggested that the majority of droughts in Turkey are of moderate severity based on SPI. They also found that while southeastern and western parts of Turkey were more stable, the central parts and few pockets in northern areas of Turkey showed lower stability against the drought impacts. Dabanlı (2018) studied the drought risk and vulnerability by using hydro-meteorological and socioeconomic data in Turkey. He found that out of 81 administrative provinces, 73 are exposed to low drought risk, 6 provinces to moderate risk and 1 province (Konya) to high drought risk.

While standard applications of drought monitoring and assessment by field data are quite prevalent (Türkeş et al. 2009; Evkaya et al. 2019; Katipoğlu et al. 2020), there is no comprehensive study evaluating the feasibility of RS data and indices for drought analysis over Turkey. Considering the large and variable climatic regions of the country, remotely sensed/modeled data coupled with classical techniques seem promising for Turkey where numerous harsh and extensive droughts have been experienced in its recent history.

Although drought events have so far been evaluated based on a number of RS data and modeled hydro-meteorological variables (Khorrami and Gunduz 2021b), there is no comprehensive survey on the feasibility and suitability of the available drought indicators in the literature. Based on this premise, we investigated the capability of GRACE-driven hydrological indices to detect and monitor two harsh dry periods (2007/2008 and 2013/2014) in Turkey. In addition, we made use of other remotely sensed and modeled drought-related parameters such as NDVI, soil moisture, ET and surface runoff to evaluate their feasibility in assisting drought surveillance over the country. Furthermore, we aimed to test the applicability and feasibility of GRACE-based indices to detect and assess the intensity and extent of droughts in semi-arid climates. Finally, we hypothesized that the GRACE-derived indices can be used to estimate the variations in the hydroclimatic extremes at large scales, and therefore, can act as surrogate indicators for the traditionally applied drought indices.

## 2. Methodology

### 2.1. Site description

Turkey is located between the latitudes 36° N and 42° N and longitudes 26° E and 45° E. The country is situated at mid-latitudes that define its climatic characteristics together with its highly variable topography. Despite its Mediterranean geographic location, where mild climatic conditions are dominant (Sensoy et al. 2008), the diversity of its topography as well as proximity to the Black Sea, Aegean Sea and the Mediterranean in the north, west and south, respectively, lead to significant variations in climatic conditions in seven different regions of the country (Figure 1). Thus, coastal zones demonstrate different characteristics from inland plateaus of central, eastern and southeastern Anatolia.

Regardless of the climatic variability of different regions of Turkey, the general climatic pattern of Turkey follows the characteristics of a generic semi-arid climate, which defines its water resources potential that in turn shapes its agriculture and industry (Selek and Aksu 2020). The variability of hydro-climatic parameters in Turkey introduces some challenges regarding water accessibility at proper times and space all over the country.

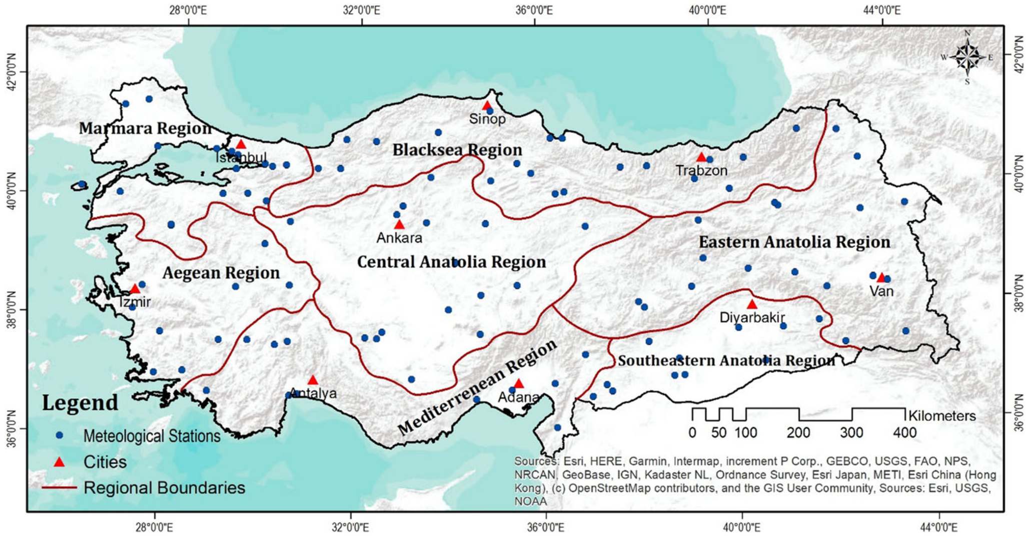


**Figure 1.** Spatial distribution of the analyzed meteorological stations over regional Turkey.

The mean annual precipitation input of Turkey is about 501 billion m$^3$ (639 mm), from which, 274 billion m$^3$ (350 mm) is lost via evaporation from the soil, water and vegetation (Okay Ahi and Jin 2019). In addition, the water demand has skyrocketed during the recent decades in the aftermath of the population increase and industrial development of the country. Consequently, it is now considered that Turkey is very sensitive to climate change impacts and is expected to face serious water scarcity problems in near future (Harmancioglu and Altinbilek 2020).

## 2.2. Data used

### 2.2.1. *In situ* climate data

Turkey benefits from a diverse network of hydro-meteorological stations administrated by the Turkish Meteorological Service (TMS). According to the TMS, Turkey has a mean annual temperature of 13.7 °C and a mean annual precipitation of 371 mm (MGM 2020). The geographic and topographic characteristics of different regions in Turkey bring about variations in the amount and distribution of climatic variables over the country. In Table 1, the basic statistics of precipitation and temperature of Turkey are given with reference to the seven regions of the country shown in Figure 1.

We used a total of 107 stations' precipitation observations to calculate traditional drought indices (Figure 1). In addition, we also utilized the long-term averages of climatic variables of precipitation ($P$) and temperature ($T$) to draw the climate graphs for the study area, which depicted the general status of the country regarding the dry and wet periods (Figure 2). According to the ombrothermic graph (Figure 2a), the monthly $P$ of the country ranges from 18 mm (in August) to 86 mm (in December) while $T$ ranges from 2 °C (in January) to 24 °C (in August). The ombrothermic graph also revealed that from July to August, Turkey experienced its highest $T$ and lowest $P$, during which the average $T$ has gone as high as 24 °C and the monthly average $P$ has fallen as low as 18.5 mm that was generally ascribed to dry seasons. Figure 2b, conversely, also showed the annual climatic situation of Turkey during the study period where two recent dry periods were observed. One of these periods prevailed from 2007 to 2008 and the other

**Table 1.** The zonal statistics of the climatic variables over Turkey.

| Variable | | Zone | Avg. | Min. | Max. | Std. Dev. |
|---|---|---|---|---|---|---|
| Monthly statistics | Precipitation (mm) | Black Sea Region (BSR) | 66.56 | 35.60 | 192.63 | 38.75 |
| | | Eastern Anatolia Region (EAR) | 50.30 | 21.43 | 101.42 | 22.04 |
| | | South-East Anatolia Region (SAR) | 47.56 | 37 | 59.52 | 9.13 |
| | | Central Anatolia Region (CAR) | 32.50 | 26.94 | 46.87 | 5.12 |
| | | Aegean Region (AR) | 56 | 36.70 | 99.63 | 19.22 |
| | | Marmara Region (MAR) | 55.50 | 37.82 | 70.50 | 10.50 |
| | | Mediterranean Region (MER) | 62.20 | 35.5 | 93.75 | 20.30 |
| | Temperature (°C) | Black Sea Region (BSR) | 12.58 | 7.01 | 14.70 | 2.15 |
| | | Eastern Anatolia Region (EAR) | 9.96 | 3.90 | 15.10 | 3.42 |

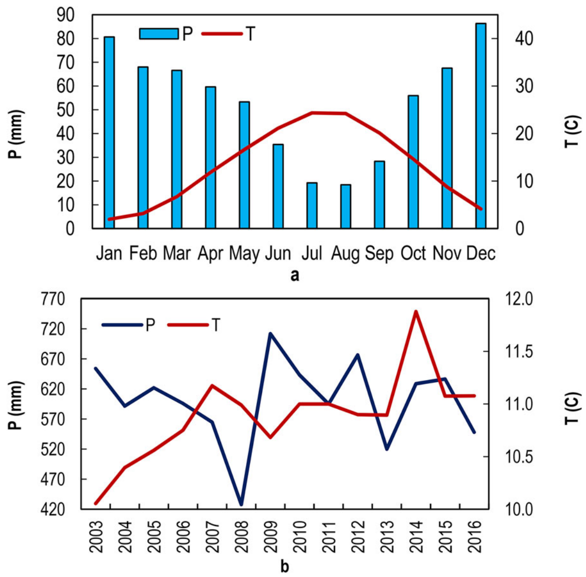


**Figure 2.** Climatic graphs of Turkey: monthly (a) and annual (b) variations of precipitation and temperature.

period from 2013 to 2014, which corresponded to the two trough points in *P* variations (428 and 520 mm in 2008 and 2013, respectively) indicating the two harsh drought events experienced in the country during 2003–2016 period.

### 2.2.2. Remotely sensed and modeled data

There are varieties of RS and modeled data sources offering global hydro-meteorological variables with different spatial and temporal resolutions. In this study, some drought-related parameters were used as drought indicators to evaluate their feasibility in the detection and monitoring of drought events over Turkey. In essence, data from two satellite missions (GRACE and Terra/Aqua) were utilized to obtain TWSA and NDVI, respectively. Moreover, modeled soil moisture values from Global Land Data Assimilation System (GLDAS) as well as Runoff (R), ET and Potential Evapotranspiration (PET) data from the ERA5 atmospheric reanalysis dataset were also used to extract auxiliary climatic information. As the fifth generation of ECMWF (the European Centre for Medium-Range Weather Forecasts), the ERA5 reanalysis data project simulates a variety of hydro-meteorological parameters integrating the historical observations into global estimates by utilizing sophisticated data assimilation models. More information can be obtained from

**Table 2.** Specifications of the datasets used in the study.

| | | Available Resolution | | |
|---|---|---|---|---|
| Data variable | Data type | Temporal | Spatial | Description and access link |
| Terrestrial Water Storage (TWS) | Satellite | Monthly (2002–2020) | 0.5° | GRACE JPL Mascon's https://earth.gsfc.nasa.gov/geo/data/grace-mascons |
| Soil Moisture Storage (SMS) | Modelled | Monthly (2000–2019) | 0.25° | GLDAS_NOAH025_M https://disc.gsfc.nasa.gov/datasets?keywords=GLDAS |
| Surface Runoff (SR) | Reanalysis | Monthly (1981–2020) | 0.1° | The Climate Data Source ERA5-Land Monthly Average Data: https://cds.climate.copernicus.eu/cdsapp#!/search?type=dataset |
| Precipitation (*P*) and Temperature (*T*) | *In situ* | Monthly (2002–2016) | – | TSMS https://mgm.gov.tr/ |
| Evapotranspiration (ET) | Reanalysis | Monthly (1981–2020) | 0.1° | The Climate Data Source ERA5-Land Monthly Average Data: https://cds.climate.copernicus.eu/cdsapp#!/search?type=dataset |
| NDVI | Satellite | Monthly (2000–2020) | 0.05° | MOD13C2 - MODIS/Terra Vegetation Indices Monthly L3 Global 0.05Deg https://ladsweb.modaps.eosdis.nasa.gov/missions-and-measurements/products/MOD13C2/ |
| Potential Reanalysis | Monthly | (1981–2020) | 0.1° | Evapotranspiration (PET) The Climate Data Source ERA5-Land Monthly Average Data: https://cds.climate.copernicus.eu/cdsapp#!/search?type=dataset |

Muñoz-Sabater et al. (2021). Table 2 illustrates the details of the datasets utilized for the analysis of this study.

Considering the different spatial resolutions of diverse datasets used, we were resampled all data using the bilinear resampling technique (Wu et al. 2008) to match the 0.5-degree resolution of GRACE TWSA in order to draw a rational analogy between the variables. Through the bilinear interpolation process, the average digital number of four adjacent cells is assigned to the cell of interest. The use of different resampling techniques depends on the user's purpose, where different advantages and disadvantages of each resampling method are to be taken into account. However, concerning the overall accuracy of these techniques, the bilinear resampling technique is known as the most appropriate method with a smoother, more accurate, and without 'stair-stepped' effect (Baboo and Devi 2010).

GRACE processing centers apply a baseline that is the mean TWS values from 2004 to 2009, to generate TWSA data. Therefore, each value represents the deviation of TWS from this baseline. We derived the anomalies of each variable according to the baseline of GRACE products.

### *2.3. Drought indices derived from GRACE*

GRACE records the gravitational signals of the Earth with an unprecedented sensitivity, which paves the way for more accurate estimations of the vertically integrated hydrological components of the water cycle over a given area (Sinha et al. 2019). These signals are recorded and later processed and translated into the variations of the TWS by three main processing centers: Center for Space Research at University of Texas, Austin (CSR), Geoforschungs Zentrum Potsdam (GFZ) and Jet Propulsion Laboratory (JPL) (Chambers 2006). GRACE TWS is a mixture of different hydrological components and is defined as follows:

$$\Delta \mathrm{TWS} = \Delta \mathrm{GWS} + \Delta \mathrm{SWE} + \Delta \mathrm{SMS} + \Delta \mathrm{SWS} \tag{1}$$

where GWS, SWE, SMS and SWS represent groundwater storage, snow water equivalent, soil moisture storage and surface water storage, respectively (Khorrami and Gunduz 2021a).

There are two approaches for translating gravitational records into TWSA values: (i) spherical harmonics (SP) and (ii) mass concentrations (Mascons). The most significant difference between these two approaches is that unlike Spherical Harmonics (SH) solutions, which are global, Mascons are regional to global solutions making them more accurate regarding the number of leakage errors in the signals (Scanlon et al. 2016).

Different techniques have been introduced to extract GRACE-based drought indices for different study areas so far. While some of the techniques used TWSA values directly (Zhao et al. 2017; Thomas et al. 2017; Yi and Wen 2016; Sun et al. 2018; Yu et al. 2019; Hosseini-Moghari et al. 2019; Nemati et al. 2019; Wang et al. 2020a; Liu et al. 2020; Shah and Mishra 2020; Yang et al. 2020), other methods took benefit of disintegrated TWSA elements to study drought events (Nair and Indu 2020; Wang et al. 2020b). Among different techniques offered by researchers, drought indices extracted directly from TWSA values are more common due to the simplicity and effectiveness of their application. In this study, we applied the GRACE TWS anomalies to calculate hydrological drought indices. We extracted the time series of TWSA using the areal mean values for each month. As there are some individual gaps in GRACE records, which hamper the continual evaluation of the values, we used the linear interpolation technique (Long et al. 2015; Yang et al. 2017a) to fill in the gaps in TWSA values.

### 2.3.1. GRACE drought severity index

GRACE drought severity index (GDSI) is a dimensionless index derived directly from GRACE TWSA values, which are capable of detecting dry and wet events. GDSI is defined as the standardized anomalies of GRACE TWSA (Zhao et al. 2017) and is formulated as:

$$\mathrm{GDSI}_{ij} = \frac{\mathrm{TWSA}_{ij} - \overline{\mathrm{TWSA}}_{j}}{\partial_j} \tag{2}$$

where $i$ denotes year ranging from 2003 to 2016; $j$ denotes month ranging from January to December; $\overline{\mathrm{TWSA}}_{j}$ and $\partial_j$ are the mean and standard deviation of TWSA in month $j$, respectively.

### 2.3.2. GRACE water storage deficit index

Water storage deficit (WSD) was developed by Thomas et al. (2014). The deviations of the water storage from the monthly climatology values (Eq. (3)) given by WSD showcase the water storage deficit and surplus in terms of negative and positive WSD values, respectively. GRACE-based water storage deficit index (WSDI) (Sinha et al. 2017; Yu et al. 2019) is calculated based on WSD values as follows:

$$\mathrm{WSD}_{ij} = \mathrm{TWSA}_{ij} - \overline{\mathrm{TWSA}_j} \tag{3}$$

$$\mathrm{WSDI}_{ij} = \frac{\mathrm{WSD}_{ij} - \mu}{\sigma} \tag{4}$$

where $\mathrm{WSD}_{ij}$ and $\mathrm{WSDI}_{ij}$ represent water storage deficit and its index for the month j of the year i respectively. $\overline{\mathrm{TWSA}_j}$ is the climatology value of month j. μ and σ denote the mean and standard deviation of the water storage deficit (WSD) time series, respectively.

## 2.4. Other RS- and model-based drought-related indices

### 2.4.1. Soil moisture index

Soil water content reflects the effect of recent precipitation along with the antecedent conditions of the soil layer (Keyantash and Dracup 2002), which indicates the water storage of soil whose variations can be used as a good indication for drought events (Sheffield et al. 2004). Soil water deficit manifests itself in crop yield and plants' conditions; hence, provides critical implications for both agriculture and water supply (Wang et al. 2011). In this study, we made use of the modeled soil moisture data from GLDAS-Noah outputs. GLDAS models soil moisture in four different depths (0–0.1, 0.1–0.4, 0.4–1.0, 1.0–2.0 m). The accumulated soil moisture of these layers was used and the standardized values as soil moisture index (SMI) of the study area were calculated using the following equation:

$$Z = \frac{X - \mu}{\sigma} \tag{5}$$

where $Z$ is the standardized variable, $x$, $\mu$ and $\sigma$ denote the variable of interest, the mean and standard deviation of the variable $x$, respectively.

### 2.4.2. Standardized runoff index

Surface runoff accounts for the volume of water that travels over the ground surface to a river or channel. Standardized runoff index (SRI) is a hydrological drought index (Shukla and Wood 2008) that is calculated in the same way as standardized precipitation index (SPI) (Sinha et al. 2019). In this study, we extracted the time series of surface runoff values from reanalysis data, and then, calculated the SRI values.

$$\mathrm{SRI} = \frac{X_i - X_j}{\sigma} \tag{6}$$

where $X_i$, $X_j$ and $\varsigma$ denote the recorded runoff in the current time scale, the average and the standard deviation of the runoff time series, respectively (Dikici and Aksel 2021).

### 2.4.3. Normalized difference vegetation index

Satellite records provide a very useful dataset of the qualitative and quantitative characteristics of vegetation coverage across large areas (Brown et al. 2008). Robust interactions between vegetation indices and climatic factors have been reported in the literature (Rundquist and Harrington 2000; Ji and Peters 2003) highlighting the effectiveness of vegetation indices in drought detection and monitoring studies. The NDVI is calculated using near-infrared and red bands according to the following equation:

$$\mathrm{NDVI} = \frac{\mathrm{Band}_{\mathrm{NIR}} - \mathrm{Band}_{\mathrm{Red}}}{\mathrm{Band}_{\mathrm{NIR}} + \mathrm{Band}_{\mathrm{Red}}} \tag{7}$$

where NIR and Red subindices stand for near-infrared and red band values, respectively. In this study, monthly NDVI products from Terra and Aqua satellites that contained the

MODIS sensors were used. The MODIS sensor on board Terra and Aqua satellites provides vegetation indices at a variety of spatiotemporal scales. In particular, we used the MOD13C2 Version 6 product from MODIS sensor, which provides a Vegetation Index (VI) value at a per pixel basis (Didan et al 2015).

#### 2.4.4. Evapotranspiration

In addition to precipitation, ET is another important component of the hydrological water cycle. During a dry condition, ET shows variations, which can be used as an indicator for a drought event. Although ET variations during a drought depend on the prevailing weather conditions, availability of water storage as well as the severity and duration of the drought (Hanson et al. 1991), the amount of ET generally shows an increase during drought periods (Stegehuis et al. 2013).

ERA5 involves the latest reanalysis in the European Centre for Medium-Range Weather Forecast's family (ECMWF) and helps to achieve a quality re-analysis of universal oceanic, atmospheric and land surface fields (Moshir Panahi et al. 2021). We used the monthly anomalies of ET values from the ERA5 reanalysis dataset as a drought indicator

### 2.5. Orthodox drought indices

Although different drought indices act as proxies for different drought types, there is a strong link between them in terms of precipitation deficit, which is a common characteristic of all drought types (Heim 2002). Traditional drought indices are generally derived from field observations of hydro-climatic variables. Field measurements guarantee the precision of these indices, thus can be used as reliable means for local-scale drought detection and monitoring as well as a robust validation tool for the assessment of the accuracy of RS and model-based techniques.

Within the scope of our analysis, we used the *in situ* observations of precipitation were used to calculate drought indices to detect the droughts over Turkey and to further validate the accuracy of our RS and model-based drought indices. To this end, we used the two well-known and commonly used traditional drought indices: (i) SPI and (ii) Standardized Precipitation-Evapotranspiration Index (SPEI). As PET values are required for the calculation of the latter, we integrated the ERA5 reanalysis datasets into the analysis to extract PET values. SPI and SPEI values were calculated in different time intervals (01, 03, 06, 09, 12 and 24 months) and then were associated with RS and model-based indices.

#### 2.5.1. Standardized precipitation index

SPI is one of the most preferred indices recommended by the 'Lincoln declaration on drought indices' (Stagge et al. 2015). Its use is encouraged by many hydro-meteorological services and researchers around the world for drought detection and monitoring (Hayes et al. 2011). SPI is calculated by fitting a gamma distribution (Hosseini-Moghari et al. 2019) to the raw precipitation data and then transforming it to a normal distribution.

$$\mathrm{SPI} = \frac{X_i - X_j}{\sigma} \tag{8}$$

where $X_i$, $X_j$ and $\varsigma$ denote the recorded precipitation in the current time scale, the average precipitation of the time series, and the standard deviation of the time series, respectively (Dikici and Aksel 2021). In this study, we calculated the SPI values using the R studio program.

### 2.5.2. Standardized precipitation-evapotranspiration index

SPEI is based on precipitation ($P$) and PET measurements (Beguería et al. 2010). Since there is no access to *in situ* PET values, a reanalysis dataset was incorporated into the analysis for obtaining PET values over Turkey. The extracted PET values were first used to derive the difference between $P$ and PET ($D$ values) according to Eq. (9) and then SPEI values were calculated in the same way as SPI, transferring $D$ values to the cumulative standard normal distribution with an average and standard deviation of 0 and 1, respectively (Hosseini-Moghari et al. 2019).

$$D_n^k = \sum_{i=0}^{k-1} \left(P_{n-i} - \mathrm{PET}_{n-i}\right) \tag{9}$$

where $D_n^k$ is the aggregated (P-PET) from the month ($n - k + 1$) to month ($n$) on time scale $k$ (Yang et al. 2017b).

## 2.6. Drought characterization

Drought can be characterized in terms of drought type, duration, magnitude, frequency, severity and spatial extent (Thomas et al. 2014). In this study, we characterized the drought events of Turkey in terms of duration, magnitude and severity. Any dry period was defined as continuous negative values of the drought index (Evkaya et al. 2019). The following drought characteristics were used in this study:

- Duration: a period of dry conditions, which lasts for at least three consecutive months (Thomas et al. 2014).
- Magnitude: the cumulative values of a given drought index within a drought event (Evkaya et al. 2019).
- Intensity: the ratio of drought magnitude to its extent (Sirdaş and Sen 2003).

Based on this fundamental, we utilized the RS datasets along with *in situ* observations to extract different drought indices to detect and characterize the recent drought events in Turkey. Figure 3 presents the methodology of the current study.

# 3. Results

## 3.1. Temporal variations of TWSA over Turkey

The TWSA values for Turkey extracted from GRACE showed a descending trend ($p < .05$) suggesting that the total water storage over the country tend to decrease (Khorrami and Gunduz 2021b). The maximum water deficits over Turkey occurred in September 2008 and September 2014 with a 19 cm water loss at each time point. Our findings were found to be consistent with that of Okay Ahi and Jin (2019). The variations of TWSA indeed resulted from the variations in hydrological water cycle components. To see the impacts of precipitation, we extracted the anomalies of precipitation using the same baseline as GRACE (i.e. the mean value from 2004 to 2009) (Moghim 2020). Then, we compared the TWSA values with Precipitation Anomalies (PA) values (Figure 4). We found a moderately strong correlation ($r = 0.64$) between the variations of TWS and $P$ over Turkey with the max PA conforming to the peaks of TWSA, which stressed the importance of the received precipitation as a major input of the hydrological cycle in the variations of the total water storage changes. The maximum deficit (39 mm) for

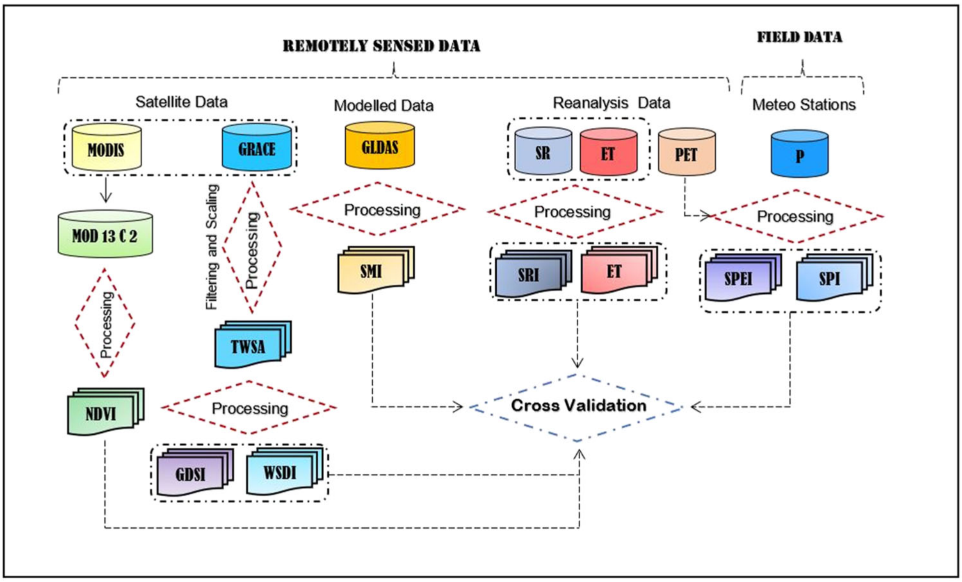


Figure 3. The graphical flowchart of the methodology.

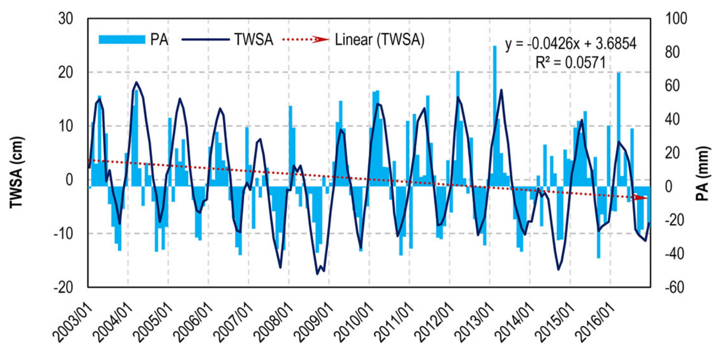


Figure 4. Temporal interactions between terrestrial water storage (TWSA) and precipitation anomalies (PA).

precipitation was seen in September 2008, which corresponded to the maximum loss of TWSA (17.54 cm) in the study area.

### 3.2. Time series of RS and model-based drought indicators

We calculated the time series of WSDI, GDSI, SMI, SRI, ET and NDVI by using the extracted values of the correspondent variables from RS and modeled datasets. Figure 5 illustrates the temporal variations of these indicators for the study area. According to the graphs, while values fluctuated monthly, the overall trends in the time series of GRACE-driven indices (GDSI and WSDI) and ET were descending, which are statistically significant ($p < .05$). The descending drought indices of WSDI and GDSI indicated that the country tends to experience drier conditions during the aforementioned period. While GDSI had its minimum value recorded in October 2007, WSDI showed the least value in February 2014.

**Table 3.** Correlation values between monthly and annual values of drought indices at different time scales.

| | | Scale | GDSI | WSDI | SMI | SRI | ET | NDVI |
|---|---|---|---|---|---|---|---|---|
| **SPI** | Monthly | 01 | 0.19 | 0.20 | 0.17 | 0.18 | −0.19 | 0.28 |
| | | 03 | 0.28 | 0.37 | 0.18 | 0.26 | −0.28 | 0.39 |
| | | 06 | 0.43 | 0.54 | 0.11 | 0.29 | −0.19 | 0.37 |
| | | 09 | 0.58 | 0.69 | 0.14 | 0.35 | −0.13 | 0.36 |
| | | 12 | 0.54 | 0.62 | 0.11 | 0.31 | −0.20 | 0.42 |
| | | 24 | 0.52 | 0.56 | 0.05 | 0.13 | −0.03 | 0.36 |
| | Annual | – | 0.66 | 0.73 | 0.75 | 0.79 | −0.46 | 0.61 |
| **SPEI** | Monthly | 01 | 0.18 | 0.20 | 0.17 | 0.19 | −0.19 | 0.28 |
| | | 03 | 0.27 | 0.36 | 0.17 | 0.26 | −0.28 | 0.39 |
| | | 06 | 0.41 | 0.53 | 0.11 | 0.46 | −0.19 | 0.37 |
| | | 09 | 0.54 | 0.66 | 0.12 | 0.34 | −0.13 | 0.34 |
| | | 12 | 0.53 | 0.62 | 0.10 | 0.31 | −0.21 | 0.43 |
| | | 24 | 0.18 | 0.20 | 0.17 | 0.19 | −0.19 | 0.28 |
| | Annual | – | 0.62 | 0.69 | 0.74 | 0.78 | −0.31 | 0.60 |

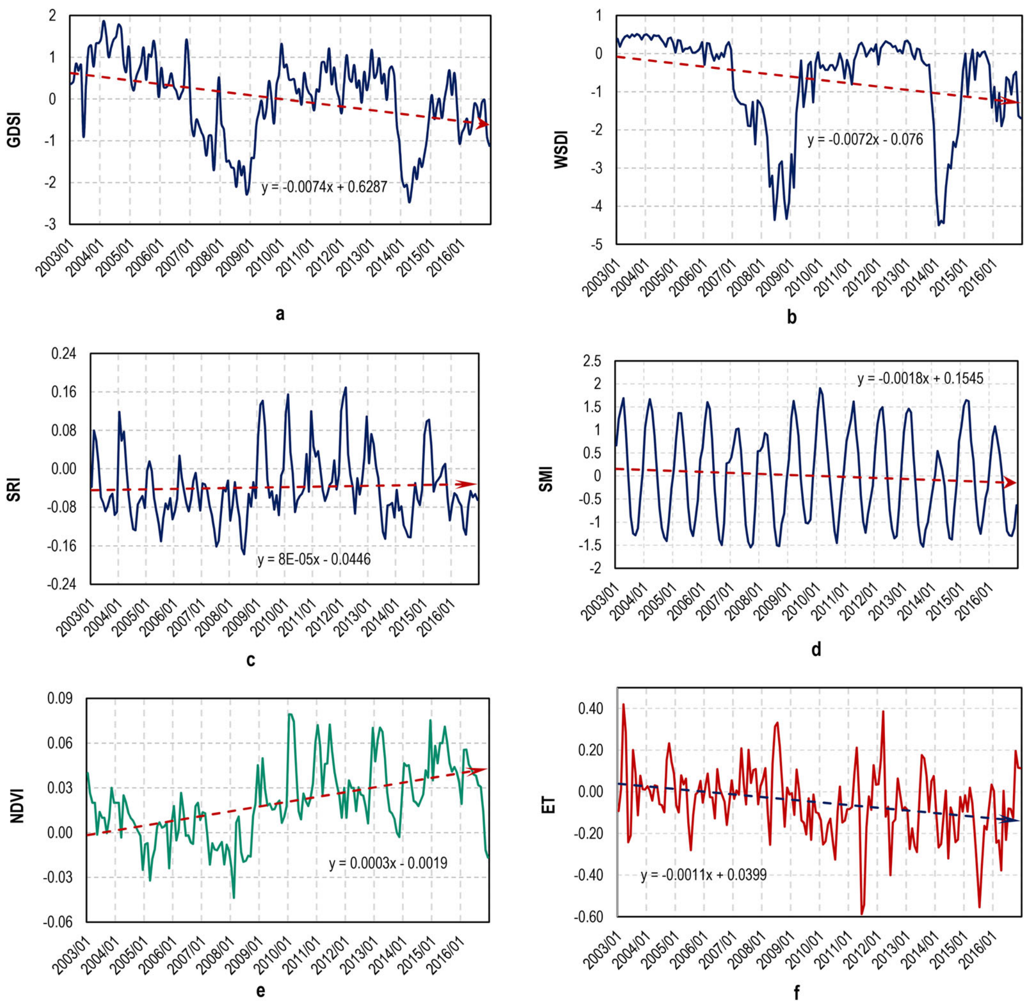


**Figure 5.** Time series of drought related indices derived from Remote Sensing (RS) data: GRACE Drought Severity Index (GDSI) (a), Water Storage Deficit Index (WSDI) (b), Surface Runoff Index (SRI) (c), Soil Moisture Index (SMI) (d), Normalized Difference Vegetation Index (NDVI) (e) and Evapotranspiration (ET) (f).

Time series of SMI, SRI and NDVI, conversely, had ascending trends, from which, only the trend of NDVI was statistically significant ($p < .05$) suggesting that it tends to increase. NDVI values manifested dramatic changes in a monthly manner with the sharpest trough recorded in February 2008. The minimum values for SMI and SRI were recorded in July 2004 and July 2008, respectively.

### 3.3. Validating the drought indices

The performance of the used RS and model-based drought indicators was evaluated in terms of point-wise linear correlations with the orthodox drought indices of SPI and SPEI in different time intervals. These well-known drought indices of SPI and SPEI are generally computed on different time scales to reflect different lags of water cycle response to precipitation anomalies (Moreira et al. 2008). In this study, we computed the SPI and SPEI values and evaluated them at different periods (Table 3) so that the drought events over Turkey were better depicted.

The results indicated that the majority of the indices correlated with SPI better than SPEI over Turkey. Among the used indicators, while GRACE-based indices (GDSI and WSDI), SMI and SRI agreed well with SPI-09, ET better agreed with SPI-03. It was also found that NDVI had its best correlation (0.43) with SPEI-12. Overall, the best performance among the indices belonged to WSDI with the maximum monthly correlation of 0.69. The differences in the algorithms and hydrologic ingredients (Liu et al. 2020) of the used parameters may influence their behaviors in detecting drought events.

The results also revealed that the used indices manifested a different behavior in detecting the annual drought events over Turkey. While WSDI had its best performance in detecting monthly dry and wet periods, SRI was the leading annual drought detector in the study area with correlation values of 0.79. The annual correlation for WSDI was also high (0.73).

### 3.4. Temporal variability of drought events

Analysis of the temporal associations between drought indices disclosed that for monthly drought detection and monitoring GRACE-driven WSDI was the best index, while for annual drought, the best results were obtained for SRI, SMI and WSDI. In this section, candidate indices for Turkey were used to show the monthly and annual time series along with SPI. According to the SPI time series (Figure 6), we found that, while there were some dry periods from 2003 to 2016, Turkey experienced extreme droughts between 2007 and 2008 and in 2014, which corresponded to the droughts detected by annual SPI. These detected dry periods were in agreement with the climate graph (Figure 2) as well as other previously published research such as Marım et al. (2008), Türkeş et al. (2009), Kurnaz (2014) and Okay Ahi and Jin (2019).

The temporal association between WSDI and the conventional indices of SPI and SPEI (Figure 6) showed that WSDI was successful in catching the profound dry (2007/2008 and 2014) and wet periods over Turkey. The annual interactions also graphically portrayed the best performance of SRI, SMI, GDSI and WSDI in defining the droughts and wet periods over the country where they were in a good harmony with the peaks and troughs of the SPI time series.

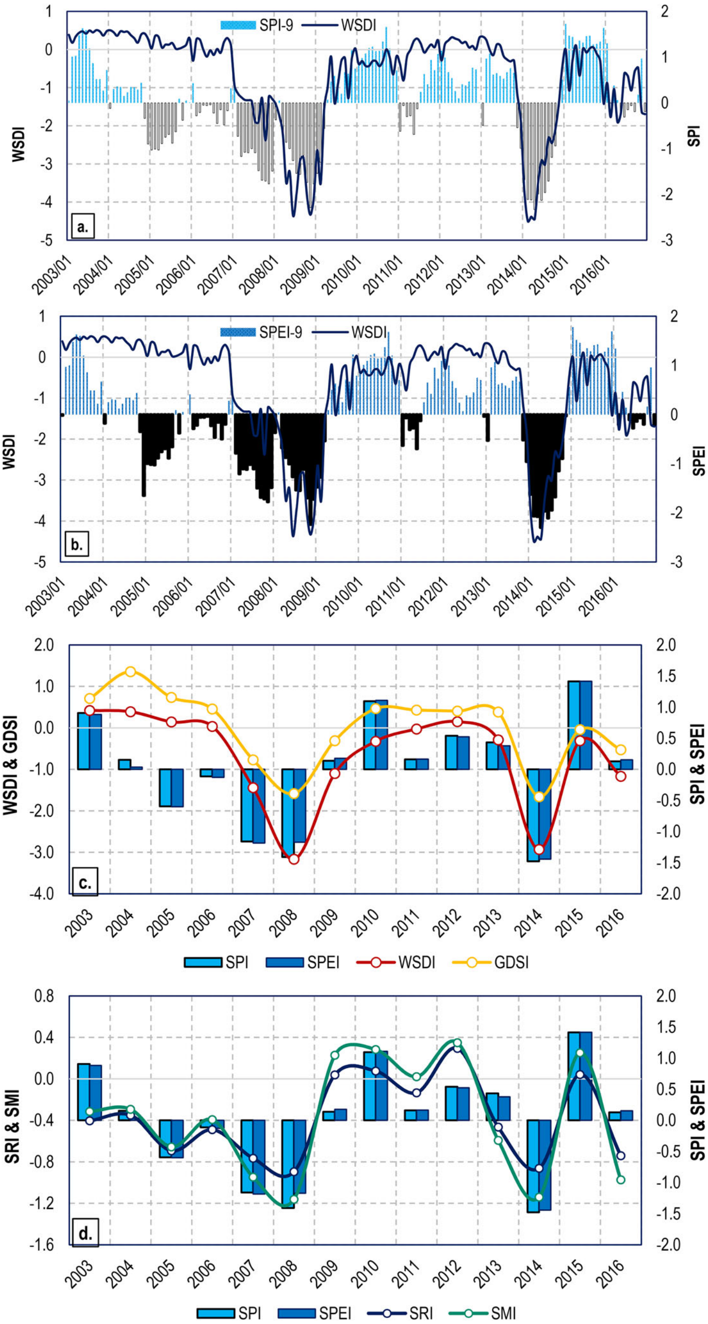


Figure 6. Temporal interactions of monthly Water Storage Deficit Index (WSDI) with Standardized Precipitation Index (SPI) and Standardized Precipitation-Evapotranspiration Index (SPEI) (a and b) and annual SPI and SPEI with WSDI, GRACE Drought Severity Index (GDSI) and Standardized Runoff Index (SRI) (c and d).

## *3.5. Spatial variability of drought*

With the aim of better visualizing the climatic situation in Turkey, we mapped the extremely dry period of the year 2008 based on WSDI and SPI values (Figure 7). We

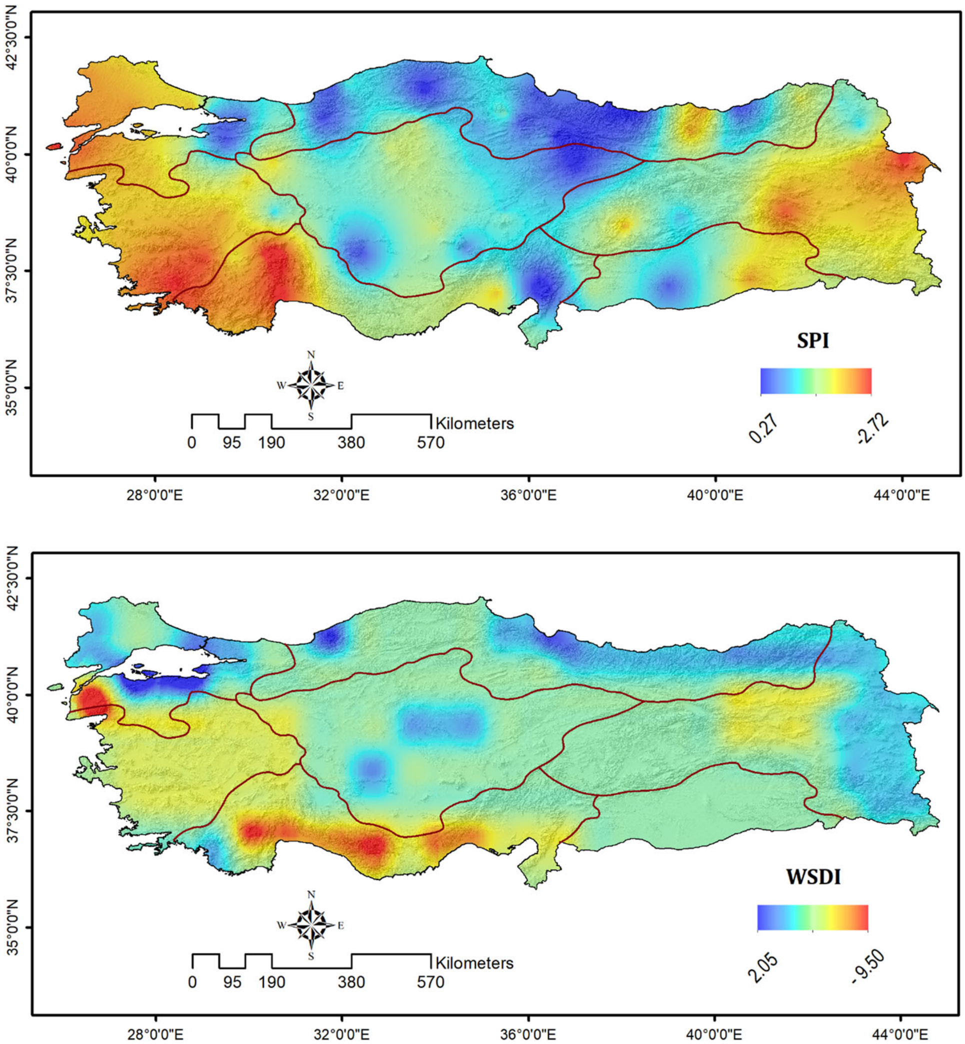


**Figure 7.** Spatial illustration of the drought of Turkey detected by Water Storage Deficit Index (WSDI) and Standardized Precipitation Index (SPI) in 2008.

specifically selected the drought event in 2008 to be visualized on the grounds of the results obtained through the SPI time series where the harshest dry period belonged to the year 2008. We generated the spatial map of the SPI based upon the Kriging interpolation technique. The visual interpretation of the maps indicated that WSDI performed very well in detecting the drought event in Turkey.

Figure 8, conversely, illustrated the interactions between WSDI and SPI indices in terms of spatial correlation value. This map showed the time series correlations achieved between the two drought indices over Turkey. The correlation map highlighted that WSDI correlated very well with SPI in the Aegean and Southeastern Anatolian regions with a spatial correlation of up to 0.72. While over Istanbul and the Black Sea region, the lowest correlation values were achieved. The correlation for the Central Anatolian region especially over the capital city of Ankara in the center was also high. These regions with high correlations were also known as regions that historically experienced the most significant droughts in Anatolia.

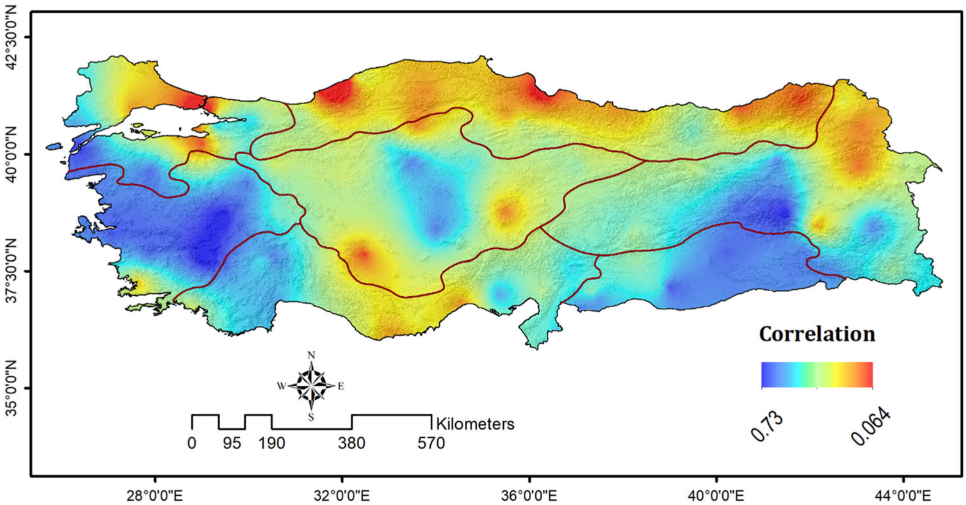


**Figure 8.** Spatial correlation between Water Storage Deficit Index (WSDI) and Standardized Precipitation Index (SPI) over Turkey.

**Table 4.** Drought magnitude classification based on Standardized Precipitation Index (SPI) and Water Storage Deficit Index (WSDI) (Sun et al. 2018).

| Class | Drought condition | SPI | WSDI |
|---|---|---|---|
| $D_0$ | No Drought | $-0.5 < S$ | $-1 < W < +1$ |
| $D_1$ | Mild Drought | $-1.0 < S \leq -0.5$ | – |
| $D_2$ | Moderate Drought | $-1.5 < S \leq -1.0$ | $-2.0 < W \leq -1.0$ |
| $D_3$ | Severe Drought | $-2.0 < S \leq -1.5$ | $-3.0 < W \leq -2.0$ |
| $D_4$ | Extreme Drought | $S \leq -2.0$ | $W \leq -3.0$ |

**Table 5.** Summary of characterizations of the drought events caught by GRACE-based Water Storage Deficit Index (WSDI).

| Event no | Drought period | Duration (Months) | Magnitude | Category | Intensity |
|---|---|---|---|---|---|
| 1 | 2006/04–2006/07 | 4 | –0.35 | $D_0$ | –0.09 |
| 2 | 2007/01–2009/11 | 35 | –68.49 | $D_4$ | –1.96 |
| 3 | 2010/01–2010/08 | 8 | –2.88 | $D_3$ | –0.36 |
| 4 | 2010/10–2011/03 | 6 | –2.40 | $D_3$ | –0.40 |
| 5 | 2013/07–2014/12 | 18 | –39.29 | $D_4$ | –2.18 |
| 6 | 2015/10–2016/12 | 15 | –15.84 | $D_4$ | –1.06 |

### *3.6. Assessment of droughts*

To characterize the recent drought events in Turkey, we used three descriptive parameters including drought duration, magnitude and intensity. The drought conditions of the recent dry periods caught by SPI and WSDI in Turkey were determined according to the classification given in Table 4.

Tables 5 and 6 portray the recent drought characteristics based on WSDI and SPI indices, respectively. According to the results, while there were seven droughts detected by SPI, the GRACE-based WSDI showed six drought events during the same study period. Furthermore, there were some temporal overlaps among the drought durations, which are clearly shown in Figure 9.

**Table 6.** Summary of characterizations of the drought events caught by Standardized Precipitation Index (SPI).

| Event no | Drought period | Duration (Months) | Magnitude | Category | Intensity |
|---|---|---|---|---|---|
| 1 | 2004/11–2005/08 | 10 | −8.90 | $D_4$ | −0.89 |
| 2 | 2006/02–2006/11 | 10 | −2.11 | $D_4$ | −0.21 |
| 3 | 2007/02–2008/01 | 12 | −14.67 | $D_4$ | −1.22 |
| 4 | 2008/03–2009/03 | 13 | −17.23 | $D_4$ | −1.33 |
| 5 | 2011/01–2011/06 | 6 | −2.08 | $D_4$ | −0.35 |
| 6 | 2013/11–2014/11 | 13 | −19.77 | $D_4$ | −1.52 |
| 7 | 2016/05–2016/09 | 5 | −0.89 | $D_1$ | −0.18 |

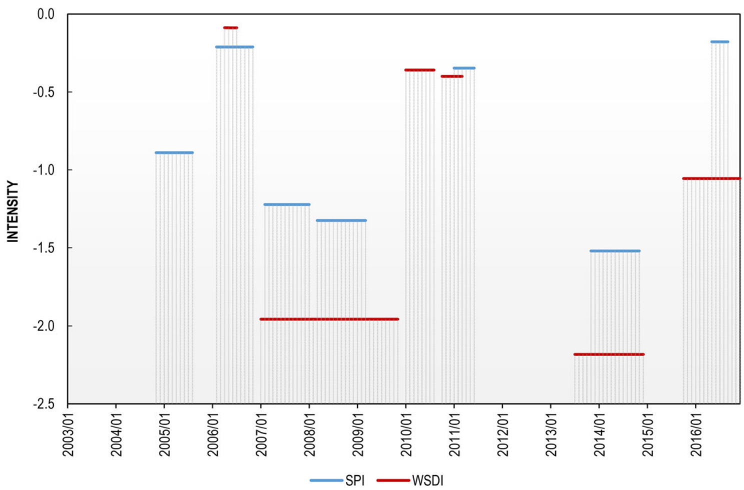


**Figure 9.** Temporal illustration of drought extent and intensity derived from Standardized Precipitation Index (SPI) and Water Storage Deficit Index (WSDI) indices.

Overall, there was no major difference between these two techniques in drought detection except for the first drought event (2004–2005) detected by SPI and the third event (2010) detected by WSDI. Thus, WSDI was considered a successful indicator in pinpointing drought events compared to the SPI results (Table 5).

The magnitude of WSDI-based droughts was almost parallel to that of SPI, which showed severe to extreme drought conditions over Turkey. The only difference in this regard was seen for the magnitude of the last drought event from May 2016 to September 2016 determined by WSDI as an extreme drought while SPI defined it as a mild condition (Figure 9).

## 4. Discussions

### *4.1. Evaluation of the GRACE-based drought indices*

The GRACE observations are sensitive to the variations in the total water storage of the Earth, which include the water stored in the soil, aquifers, as well as surface water-bearing bodies. Therefore, it can be used to analyze different types of droughts (Vishwakarma 2020). Different GRACE-based drought indices are essentially based on the GRACE-observed TWSA values, thus the characteristics of the TWSA over a region define, to a great extent, the behavior of the GRACE-based drought indices. The decreasing variations of the GRACE-derived TWSA over Turkey suggest that the country became drier during the study period between 2003 and 2016 (Figure 4). The overall descending trend of the TWSA graph is also manifested in the time-series graphs of the GRACE-based drought indices of WSDI and GDSI (Figure 5). The results of this study reveal that the GRACE-based indices act quite well in detecting the major drought (Nigatu et al (2021) events experienced over Turkey. The performance of the WSDI index turned out to be the highest among different indices used for this purpose over the study area. This finding is in accordance with the findings of Sinha et al (2017), Sun et al (2018), Yu et al (2019) and Nigatu et al (2021).

### 4.2. The climatic heterogeneity of Turkey and its impacts on the results

Turkey hosts different geographic regions with diverse topographic and climatic features. This diversity of the climate yields spatio-temporal heterogeneity of different hydrometeorological variables over different regions of the country triggering some challenges when a countrywide study is carried out. Therefore, the climatic differences among different regions over the country should be included in the interpretation and discussion of the results.

The time series of the spectral indices of drought were generated using the area-mean values for each month. The overall trends for the GRACE-based drought indices (GDSI and WSDI) were descending suggesting that Turkey tended to lose water storage mainly due to the climate change impacts (Okay Ahi and Jin 2019; Khorrami and Gunduz 2021a). The trendlines of the other RS and model-based indices (e.g. NDVI and SMI), however, did not comply with the GRACE-derived indices in terms of temporal trends where the soil moisture and vegetation coverage manifest increasing trends, which was against what one could expect for the study area. These discrepancies may stem from a set of factors such as the nature of the datasets used in the study as well as the data analysis approaches. From this viewpoint and considering the characteristics of the study area and the way of data analysis (point-wise data analysis coupled with spatial interpolation), the mismatches between the different indices used in this study can be explained. The study was performed in a very heterogeneous location, where deep discrepancies in the climatic status of different regions were experienced (Türkeş et al. 1995) and this approach culminated in the mismatches in the overall trends and spatial distribution of indices over Turkey. Moreover, the applied data with different spatio-temporal characteristics contributed to the variations and mismatches of the results. It should also be noted that the drought analysis based on remotely sensed data is to some extent limited by not only the accuracy of the datasets but also their spatial resolutions. These issues might result in the partial capturing performance of spatial heterogeneity. Nevertheless, GRACE-like datasets are still invaluable tools in the large-scale analysis of hydrometeorological events.

### 4.3. The geographic distribution of the drought event over Turkey

Using the minimum values of the candidate indices, the spatial maps of the 2008 drought event for Turkey were generated. According to the WSDI map (Figure 7), during the 2008 drought event over Turkey, the most dramatic situation was experienced in the coastal regions of the Black Sea, Istanbul metropolitan area and a wide area in Central Anatolia (center of the country) (Khorrami and Gunduz 2021b). Although there were some zonal mismatches between the distribution of the drought values from SPI and WSDI (Figure 8), which may stem from the technical issues regarding the resolution of the data as well as the data processing and analysis issues (Yu et al. 2019), the overall spatial distribution of WSDI values corresponded quite well with that of SPI portraying the zonal status of the climatic situation of Turkey during the harshest dry events of the year 2008 (Figure 8).

The dissimilarities of the drought maps may also refer to the way the drought index values were calculated and visualized. The GRACE-derived WSDI map was generated using the resampled gridded data, while for generating SPI surface, spatial interpolation was implemented. Resampling and interpolation techniques were associated with different uncertainties (Gardner 2003), which in turn altered the accuracy level of the analysis and outputs. Furthermore, for a better depiction of droughts based on SPI, the temporal range of the used precipitation data is a critical issue where longer data means more accurate results (Svoboda and Fuchs 2017). Taking these technical issues into account, it can be stated that small mismatches observed in the spatial illustration of droughts over Turkey were inevitable.

## 5. Conclusions

Drought studies are traditionally based on field observations of hydro-meteorological parameters. These are typically limited in time and geographic space, which lowers the spatial and temporal accuracy of the studies. In this study, we used the remotely sensed and simulated data in an integrated manner to evaluate the recent droughts over the semi-arid climatic region of Turkey, for which there is no comprehensive comparative study from the viewpoint of the effectiveness of different drought indices available for the scientific community use.

The results indicated that among different RS indices, notwithstanding its coarse resolution estimates, the GRACE-driven WSDI index had the best performance in detecting the monthly dry periods while SRI relatively outperformed WSDI in the detection of yearly droughts in Turkey from 2003 to 2016. The correlations achieved between used indices indicated that RS and model-based indicators had, in general, better agreement with SPI rather than SPEI even though the differences between the correlation values achieved for these two indices were not so high. This can be ascribed to the fact that SPI was more dependent on precipitation than SPEI and the fluctuations of precipitation were more influential on the climatic condition of Turkey, which made SPI perform more effectively.

Although GRACE signals were more sensitive to hydrological drought conditions rather than other types, our findings emphasized the high capability of the GRACE-driven WSDI for the determination and evaluation of the meteorological droughts in Turkey. Therefore, it can be claimed that WSDI can be used as a proxy for detecting and assessing meteorological droughts in Turkey. Especially for local studies over the Aegean and Southeastern Anatolian regions, GRACE-based WSDI performed very well suggesting that it can be replaced with traditional SPI and SPEI indices in drought monitoring studies.

The main limitation of the study, however, was associated with the coarse spatial resolution of GRACE grids. This handicap interrupted accurate estimations of TWSA, and thus, lowered the accuracy of the TWSA related studies using GRACE. GRACE data also suffer from some errors called ‘leakage errors’, which refer to the leaking signals from the surrounding areas or water bodies hazing the accuracy of the analysis. Nevertheless, with the application of streamlined processing techniques by the data producer on one hand and the use of downscaling techniques by end-users on the other hand, it is believed that GRACE TWSA estimates will improve significantly so that more precise drought studies will be possible in the future.

## Author's contributions

Behnam Khorrami: Conceptualization, Methodology, Data collection and analysis, Writing; Orhan Gündüz: Methodology, Review and Editing.

## Author's statements

The authors would like to state that there are no financial interests or connections that might raise the question of bias in the work reported or the conclusions, implications or opinions stated.

## Disclosure statement

No potential conflict of interest was reported by the authors.

## Funding

This research did not receive any specific grant from funding agencies in the public, commercial or not-for-profit sectors.

## ORCID

Behnam Khorrami http://orcid.org/0000-0003-3265-372X
Orhan Gündüz http://orcid.org/0000-0001-6302-0277

## Data availability statement

The data that support the findings of this study are available from the corresponding author upon reasonable request.

## References

Baboo SS, Devi MR. 2010. An analysis of different resampling methods in Coimbatore, district. Glob J Comput Sci Technol. 10(15):61–66.

Beguería S, Vicente-Serrano SM, Angulo-Martínez M. 2010. A multiscalar global drought dataset: the SPEI base: a new gridded product for the analysis of drought variability and impacts. Bull Am Meteorol Soc. 91(10):1351–1356.

Brown JF, Wardlow BD, Tadesse T, Hayes MJ, Reed BC. 2008. The vegetation drought response index (VegDRI): a new integrated approach for monitoring drought stress in vegetation. GISci Remote Sens. 45(1):16–46.

Chambers DP. 2006. Evaluation of new GRACE time-variable gravity data over the ocean. Geophys Res Lett. 33(17) L17603.

Cui A, Li J, Zhou Q, Wu G, Li Q. 2019. Hydrological drought measurement using GRACE terrestrial water storage anomaly. IGARSS 2019-2019 Proceedings of the IEEE International Geoscience and Remote Sensing Symposium. Japan: Yokohama; p. 9914–9917.

Dabanli, I. 2018. Drought hazard, vulnerability, and risk assessment in Turkey. Arab J Geosci. 11:538.

Dabanlı İ, Mishra AK, Şen Z. 2017. Long-term spatio-temporal drought variability in Turkey. J Hydrol. 552:779–792.

Dharpure JK, Goswami A, Patel A, Kulkarni AV, Meloth T. 2020. Drought characterization using the combined terrestrial evapotranspiration index over the Indus, Ganga and Brahmaputra river basins. Geocarto Int. 1–25. Ahead-of-print.

Didan K, Munoz AB, Solano R, Huete A. 2015. MODIS vegetation index user's guide (MOD13 series). Tucson (AZ): University of Arizona, Vegetation Index and Phenology Lab.
Dikici M, Aksel M. 2021. Comparison of drought indices in the case of the Ceyhan Basin. Int J Environ Geoinformatics. 8(2):113–125.
Dutta D, Kundu A, Patel NR, Saha SK, Siddiqui AR. 2015. Assessment of agricultural drought in Rajasthan (India) using RS derived Vegetation Condition Index (VCI) and Standardized Precipitation Index (SPI). Egypt J Remote Sens Space Sci. 18(1):53–63.
Evkaya O, Yozgatligil C, Selcuk-Kestel AS. 2019. Drought analysis using copula approach: a case study for Turkey. Commun Stat Case Stud Data Anal Appl. 5(3):243–260.
Gardner JL. 2003. Uncertainties in interpolated spectral data. J Res Natl Inst Stand Technol. 108(1):69–78.
Gu Y, Brown JF, Verdin JP, Wardlow B. 2007. A five-year analysis of MODIS NDVI and NDWI for grassland drought assessment over the central Great Plains of the United States. Geophys Res Lett. 34(6):L06407.
Hanson RL, In Paulson RW, Chase EB, Roberts RS, Moody DW. 1991. Evapotranspiration and droughts compilers, national water summary 1988-89 - Hydrologic events and floods and droughts. U.S. Geological Survey Water-Supply Paper 2375, Reston (VA); p. 99–104.
Harmancioglu NB, Altinbilek D, editors. 2020. Water Resources of Turkey. Cham (Switzerland): Springer International Publishing.
Hayes M, Svoboda M, Wall N, Widhalm M. 2011. The Lincoln declaration on drought indices: universal meteorological drought index recommended. Bull Am Meteorol Soc. 92(4):485–488.
Heim RR. Jr. 2002. A review of twentieth-century drought indices used in the United States. Bull Am Meteorol Soc. 83(8):1149–1166.
Hosseini-Moghari SM, Araghinejad S. 2015. Monthly and seasonal drought forecasting using statistical neural networks. Environ Earth Sci. 74(1):397–412.
Hosseini-Moghari SM, Araghinejad S, Ebrahimi K, Tourian MJ. 2019. Introducing modified total storage deficit index (MTSDI) for drought monitoring using GRACE observations. Ecol Indic. 101:465–475.
Ji L, Peters AJ. 2003. Assessing vegetation response to drought in the northern great plains using vegetation and drought indices. Remote Sens Environ. 87(1):85–98.
Katipoğlu OM, Acar R, Şengül S. 2020. Comparison of meteorological indices for drought monitoring and evaluating: a case study from Euphrates basin, Turkey. J Water Clim Chang. 11(S1):29–43.
Keyantash J, Dracup JA. 2002. The quantification of drought: an evaluation of drought indices. Bull Am Meteorol Soc. 83(8):1167–1180.
Khorrami B, Gündüz O. 2019. Analyses of meteorological drought and its impacts on groundwater fluctuations, a case study: Marand Plain (Iran). Pamukkale J Eng Sci. 25(6):711–717.
Khorrami B, Gunduz O. 2021a. Evaluation of the temporal variations of groundwater storage and its interactions with climatic variables using GRACE data and hydrological models: a study from Turkey. Hydrol Process. 35(3):e14076.
Khorrami B, Gunduz O. 2021b. An enhanced water storage deficit index (EWSDI) for drought detection using GRACE gravity estimates. J Hydrol. 603:126812.
Klisch A, Atzberger C. 2016. Operational drought monitoring in Kenya using MODIS NDVI time series. Remote Sens. 8(4):267.
Kurnaz L. 2014. Drought in Turkey. İstanbul Policy Center, Sabancı Üniversitesi-İstanbul. https://ipc.sabanciuniv.edu/Content/Images/CKeditorImages/20200323-16034017.pdf.
Li B, Rodell M, Zaitchik BF, Reichle RH, Koster RD, van Dam TM. 2012. Assimilation of GRACE terrestrial water storage into a land surface model: evaluation and potential value for drought monitoring in western and central Europe. J Hydrol. 446–447:103–115.
Liu X, Feng X, Ciais P, Fu B, Hu B, Sun Z. 2020. GRACE satellite-based drought index indicating increased impact of drought over major basins in China during 2002–2017. Agric For Meteorol. 291:108057.
Long D, Yang Y, Wada Y, Hong Y, Liang W, Chen Y, Yong B, Hou A, Wei J, Chen L. 2015. Deriving scaling factors using a global hydrological model to restore GRACE total water storage changes for China's Yangtze River Basin. Remote Sens Environ. 168:177–193.
Marım G, Sensoy A, Sorman A, Sorman A. 2008. Yukarı Fırat Havzası İçin Elde Edilen Kar Çekilme Eğrilerinin Zamansal Analizi ve Modelleme Çalışmaları. Proceedings of Kar Hidrolojisi Konferansı, DSİ VIII. Regional Directorate, Atatürk University, Erzurum, Turkey (original in Turkish)
MGM. 2020. Turkish State Meteorological Service [MGM]. Official Statistics. [2020 March 05]. https://www.mgm.gov.tr/veridegerlendirme/il-ve-ilceler-istatistik.aspx.
Moghim S. 2020. Assessment of water storage changes using GRACE and GLDAS. Water Resour Manage. 34(2):685–697.

Moreira EE, Coelho CA, Paulo AA, Pereira LS, Mexia JT. 2008. SPI-based drought category prediction using log-linear models. J Hydrol. 354(1–4):116–130.
Moshir Panahi D, Sadeghi Tabas S, Kalantari Z, Ferreira CSS, Zahabiyoun B. 2021. Spatio-temporal assessment of global gridded evapotranspiration datasets across Iran. Remote Sens. 13(9):1816.
Muñoz-Sabater J, Dutra E, Agustí-Panareda A, Albergel C, Arduini G, Balsamo G, Boussetta S, Choulga M, Harrigan S, Hersbach H, et al. 2021. ERA5-Land: a state-of-the-art global reanalysis dataset for land applications. Earth Syst Sci Data. 13(9):4349–4383.
Nair AS, Indu J. 2020. Changing groundwater storage trend of India after severe drought. Int J Remote Sens. 41(19):7565–7584.
Nemati A, Ghoreishi Najafabadi SH, Joodaki G, Mousavi Nadoushani SS. 2019. Monitoring and analysis of drought using gravity recovery and climate experiment (GRACE). Hydrology. 6(3):75.
Nigatu ZM, Fan D, You W, Melesse AM. 2021. Hydroclimatic extremes evaluation using GRACE/GRACE-FO and multidecadal climatic variables over the Nile river basin. Remote Sens. 13(4):651.
Okay Ahi G, Jin S. 2019. Hydrologic mass changes and their implications in Mediterranean-climate Turkey from GRACE measurements. Remote Sens. 11(2):120.
Ramillien G, Famiglietti JS, Wahr J. 2008. Detection of continental hydrology and glaciology signals from GRACE: a review. Surv Geophys. 29(4–5):361–374.
Rundquist BC, Harrington JA Jr. 2000. The effects of climatic factors on vegetation dynamics of tallgrass and shortgrass cover. GeoCarto Int. 15(3):33–36.
Sattar MN, Jehanzaib M, Kim JE, Kwon HH, Kim TW. 2020. Application of the hidden Markov Bayesian classifier and propagation concept for probabilistic assessment of meteorological and hydrological droughts in South Korea. Atmosphere. 11(9):1000.
Scanlon BR, Zhang Z, Save H, Wiese DN, Landerer FW, Long D, Longuevergne L, Chen J. 2016. Global evaluation of new GRACE mascon products for hydrologic applications. Water Resour Res. 52(12):9412–9429.
Selek B, Aksu H. 2020. Water resources potential of Turkey. In: Water Resources of Turkey. Cham: Springer; p. 241–256.
Sensoy S, Demircan M, Ulupinar Y, Balta I. 2008. Climate of Turkey. Ankara (Turkey): Turkish State Meteorological Service; p. 401.
Shah D, Mishra V. 2020. Integrated Drought Index (IDI) for drought monitoring and assessment in India. Water Resour Res. 56(2):e2019WR026284.
Sheffield J, Goteti G, Wen F, Wood EF. 2004. A simulated soil moisture based drought analysis for the United States. J Geophys Res. 109(D24):D24108.
Shukla S, Wood AW. 2008. Use of a standardized runoff index for characterizing hydrologic drought. Geophys Res Lett. 35(2):L02405.
Simsek O, Cakmak B. 2010. Drought analysis for 2007-2008 agricultural year of Turkey. Tekirdağ Ziraat Fakültesi Dergisi. 7(3):99–109.
Sinha D, Syed TH, Famiglietti JS, Reager JT, Thomas RC. 2017. Characterizing drought in India using GRACE observations of terrestrial water storage deficit. J Hydrometeorol. 18(2):381–396.
Sinha D, Syed TH, Reager JT. 2019. Utilizing combined deviations of precipitation and GRACE-based terrestrial water storage as a metric for drought characterization: a case study over major Indian river basins. J Hydrol. 572:294–307.
Sirdaş S, Sen Z. 2003. Spatio-temporal drought analysis in the Trakya region, Turkey. Hydrol Sci J. 48(5):809–820.
Smakhtin VU, Hughes DA. 2007. Automated estimation and analyses of meteorological drought characteristics from monthly rainfall data. Environ Modell Softw. 22(6):880–890.
Sönmez FK, Kömüscü AÜ, Erkan A, Turgu E. 2005. An analysis of spatial and temporal dimension of drought vulnerability in Turkey using the standardized precipitation index. Nat Hazards. 35(2):243–264.
Souza A, Neto AR, de Souza LL. 2021. Soil moisture-based index for agricultural drought assessment: SMADI application in Pernambuco State-Brazil. Remote Sens Environ. 252:112124.
Stagge JH, Kohn I, Tallaksen LM, Stahl K. 2015. Modeling drought impact occurrence based on meteorological drought indices in Europe. J Hydrol. 530:37–50.
Stegehuis AI, Vautard R, Ciais P, Teuling AJ, Jung M, Yiou P. 2013. Summer temperatures in Europe and land heat fluxes in observation-based data and regional climate model simulations. Clim Dyn. 41(2):455–477.
Sun Z, Zhu X, Pan Y, Zhang J, Liu X. 2018. Drought evaluation using the GRACE terrestrial water storage deficit over the Yangtze River Basin, China. Sci Total Environ. 634:727–738.

Svoboda M, Fuchs B. 2017. Handbook of drought indicators and indices. Geneva: Integrated Drought Management Tools and Guidelines Series; p. 155–208.
Thomas AC, Reager JT, Famiglietti JS, Rodell M. 2014. A GRACE-based water storage deficit approach for hydrological drought characterization. Geophys Res Lett. 41(5):1537–1545.
Thomas BF, Famiglietti JS, Landerer FW, Wiese DN, Molotch NP, Argus DF. 2017. GRACE groundwater drought index: evaluation of California Central Valley groundwater drought. Remote Sens Environ. 198:384–392.
Türkeş M, Koç T, Sariş F. 2009. Spatiotemporal variability of precipitation total series over Turkey. Int J Climatol. 29(8):1056–1074.
Türkeş M, Sümer UM, Kiliç G. 1995. Variations and trends in annual mean air temperatures in Turkey with respect to climatic variability. Int J Climatol. 15(5):557–569.
Vishwakarma BD. 2020. Monitoring Droughts From GRACE. Front Environ Sci. 8:584690.
Wang A, Lettenmaier DP, Sheffield J. 2011. Soil moisture drought in China, 1950–2006. J Clim. 24(13): 3257–3271.
Wang F, Wang Z, Yang H, Di D, Zhao Y, Liang Q. 2020b. Utilizing GRACE-based groundwater drought index for drought characterization and teleconnection factors analysis in the North China Plain. J Hydrol. 585:124849.
Wang J, Chen Y, Wang Z, Shang P. 2020a. Drought evaluation over Yangtze River basin based on weighted water storage deficit. J Hydrol. 591:125283.
Wilhite DA. 2005. Drought and water crises: science, technology, and management issues. Vol. 86. Boca Raton (FL): CRC Press.
Wu S, Li J, Huang GH. 2008. A study on DEM-derived primary topographic attributes for hydrologic applications: sensitivity to elevation data resolution. Appl Geogr. 28(3):210–223.
Xie Y, Wang P, Bai X, Khan J, Zhang S, Li L, Wang L. 2017. Assimilation of the leaf area index and vegetation temperature condition index for winter wheat yield estimation using Landsat imagery and the CERES-Wheat model. Agric For Meteorol. 246:194–206.
Yang P, Xia J, Zhan C, Qiao Y, Wang Y. 2017a. Monitoring the spatio-temporal changes of terrestrial water storage using GRACE data in the Tarim River basin between 2002 and 2015. Sci Total Environ. 595:218–228.
Yang P, Zhang Y, Xia J, Sun S. 2020. Identification of drought events in the major basins of Central Asia based on a combined climatological deviation index from GRACE measurements. Atmos Res. 244: 105105.
Yang Q, Li M, Zheng Z, Ma Z. 2017b. Regional applicability of seven meteorological drought indices in China. Sci China Earth Sci. 60(4):745–760.
Yi H, Wen L. 2016. Satellite gravity measurement monitoring terrestrial water storage change and drought in the continental United States. Sci Rep. 6:19909.
Yu W, Li Y, Cao Y, Schillerberg T. 2019. Drought assessment using GRACE terrestrial water storage deficit in Mongolia from 2002 to 2017. Water. 11(6):1301.
Zhao M, Geruo A, Velicogna I, Kimball JS. 2017. A global gridded dataset of GRACE drought severity index for 2002–14: comparison with PDSI and SPEI and a case study of the Australia millennium drought. J Hydrometeorol. 18(8):2117–2129.